Progress In Electromagnetics Research M, Vol. 6, 107–122, 2009

RECONSTRUCTION PERMITTIVITY TENSOR AND PRINCIPAL AXIS FOR UNIAXIAL MEDIUM IN MICROWAVE BAND

B. Wei, F. Wang, and D. B. Ge

Physics Department
Xidian University
Xi'an, Shaanxi 710071, China

Abstract—The relationship of permittivity tensor of anisotropic medium in principal coordinate system and laboratory coordinate system is given. The characteristic of permittivity tensor of uniaxial anisotropic medium in the laboratory coordinate system is discussed. The transverse permittivity of an anisotropic plate is reconstructed in laboratory coordinate system based on the resonance and polarization characteristics of backscattering radar cross section (RCS) in wide band. Then, a new scheme of reconstructing the principal axis direction for a uniaxial sample plate is proposed, subject to the principal axis is unknown. The backscattering characteristics of a sample plate are discussed when the electromagnetic (EM) wave of different polarization is incident perpendicular to the sample plate. Three sample plates, which are cut perpendicularly to the x', y', and z' axes in the laboratory coordinate system, are required. A numerical reconstruction example is given to demonstrate the availability of presented scheme.

1. INTRODUCTION

In recent years, there have been growing interests in the interactions between electromagnetic fields and anisotropic media [1–14], and the measurement of constitutive parameters of anisotropic medium at microwave frequencies [15–19], primarily because of its wide applications in the design and analysis of various novel antenna and microwave devices of high performance. Drude studied the inverse problem of scattering with respect to optical band. Fedorov

Corresponding author: B. Wei (bwei@xidian.edu.cn).

et al. considered the inverse problem for homogeneous absorbing crystals. Borzdov studied the reflection and transmission operators of a multilayer structure consisting of anisotropic media and reconstruction of material parameters for layer bianisotropic media. In these studies the direction of the principal axis of the anisotropic medium was supposed already known. With the development of the technology, the reconstruction of anisotropic constructive parameters and principal axis in three dimensional problem is of practically usage in microwave band. In this paper, we reconstructed the transverse permittivity of an anisotropic plate in laboratory coordinate system based on the resonance and polarization characteristics of backscattering radar cross section (RCS) in wide band. A new reconstruction scheme of principal axis direction for a uniaxial medium in laboratory coordinate system is given based on the analysis of the backscattering when the electromagnetic (EM) wave is incident perpendicular to a uniaxial plate. Three sample plates, which are cut perpendicularly to the x', y', and z' axes in the laboratory coordinate system, are required. Numerical examples are given to show the availability of presented reconstruction scheme.

2. THE PERMITTIVITY TENSOR IN THE LABORATORY COORDINATE SYSTEM

The constitutive relations for an electrically anisotropic uniaxial medium can be written as

$$\mathbf{D} = \boldsymbol{\varepsilon} \cdot \mathbf{E} \tag{1}$$

where $\mathbf{D}$, $\mathbf{E}$ and $\boldsymbol{\varepsilon}$ are the electric displacement, the electric field strength and the permittivity tensor, respectively.

The permittivity tensor has the simplest expression in principal system (xyz system). However, the measurement is usually performed in the laboratory coordinate system ($x'y'z'$ system). The transformation from the principal system to the laboratory system is as follows [20]:

$$\boldsymbol{\varepsilon}' = \mathbf{U} \cdot \boldsymbol{\varepsilon} \cdot \mathbf{U}^{\mathbf{T}} \quad \mathbf{U} = \begin{bmatrix} \cos\varphi & -\sin\varphi & 0 \\ \cos\theta\sin\varphi & \cos\theta\cos\varphi & -\sin\theta \\ \sin\theta\sin\varphi & \sin\theta\cos\varphi & \cos\theta \end{bmatrix} \tag{2}$$

where $\boldsymbol{\varepsilon}$ and $\boldsymbol{\varepsilon'}$ are the permittivity tensor in principal and laboratory systems, respectively. $\mathbf{U}$ is the transformation matrix; $\mathbf{U}^{\mathbf{T}}$ is the transpose matrix of $\mathbf{U}$. θ is the angle of positive z axis with respect to the positive z' axis; φ is the angle of the projection of z axis with respect to y' axis, as shown in Figure 1; and $\theta \in [0, \pi]$, $\varphi \in [0, 2\pi]$.

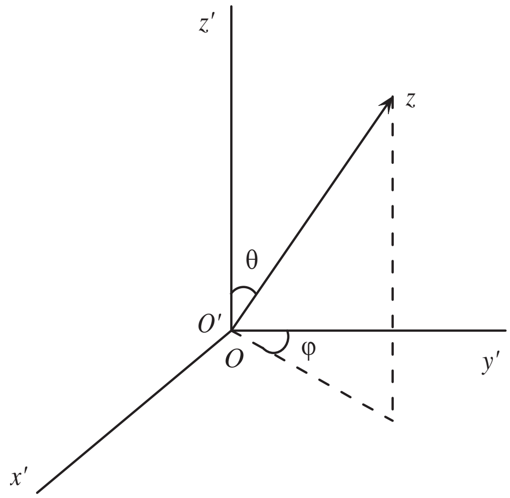

Figure 1. The orientation angle of z' axis in principal system.

The permittivity tensor of uniaxial medium in principal system is $\boldsymbol{\varepsilon} = \mathrm{diag}\,(\varepsilon, \varepsilon, \varepsilon_z)$, according to Equation (2) the permittivity tensor in laboratory coordinate system can be written as

$$\boldsymbol{\varepsilon'} = \begin{bmatrix} \varepsilon & 0 & 0 \\ 0 & \varepsilon\cos^2\theta + \varepsilon_z\sin^2\theta & (\varepsilon - \varepsilon_z)\sin\theta\cos\theta \\ 0 & (\varepsilon - \varepsilon_z)\sin\theta\cos\theta & \varepsilon\sin^2\theta + \varepsilon_z\cos^2\theta \end{bmatrix} = \begin{bmatrix} \varepsilon & 0 & 0 \\ 0 & \varepsilon_{yy} & \varepsilon_{yz} \\ 0 & \varepsilon_{zy} & \varepsilon_{zz} \end{bmatrix} \quad (3)$$

It can be seen from Equation (3) that the permittivity tensor in laboratory coordinate system is independent of angle φ. It can be observed from $\mathbf{D} = \boldsymbol{\varepsilon}' \cdot \mathbf{E}$ that there is no cross polarization component if the external field is parallel to x' axis, and the cross polarization components appear if the external field is parallel to y' or z' axis.

3. CHARACTERISTICS OF THE BACKSCATTERING RCS OF AN ELECTRICALLY ANISOTROPIC PLATE

In this paper, the scattering characteristics of the anisotropic medium are computed by the Finite Difference Time Domain (FDTD) method [21, 22]. The dispersion of the permittivity tensor is not taken into account because the scattering of three-dimensional anisotropic media is very complicated.

The geometry of an anisotropic plate and the direction of the incident wave are shown in Figure 2. First, consider the situation when the principal and laboratory systems are superposition. The

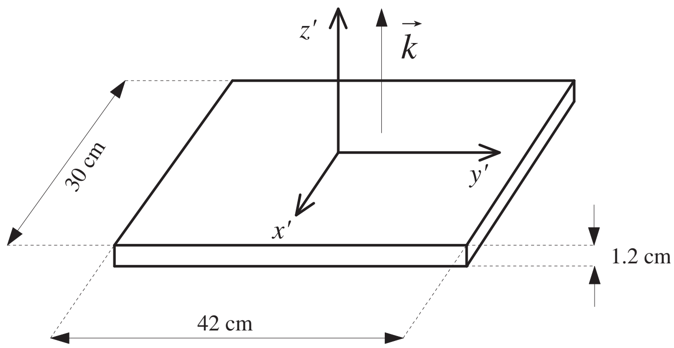

Figure 2. Geometry of an anisotropic plate.

dimension of the plate is 30 cm × 42 cm × 1.2 cm; the permittivity tensor and the conductivity tensor are $\boldsymbol{\varepsilon} = \varepsilon_0 \mathrm{diag}\,(4.0,\, 3.0,\, 2.0)$ and $\boldsymbol{\sigma} = \mathrm{diag}\,(0.05,\, 0.04,\, 0.03)$, respectively. The backscattering RCS of the anisotropic plate of different polarization are shown in Figure 3(a). The real line, star, triangle and dot show the angle α (the angle of electric field of the incident wave with respect to the positive direction of the x' axis) which are 0°, 30°, 60° and 90°, respectively.

Then consider the situation that the principal and laboratory systems are not superposition. The orientation angles of the z axis in laboratory system are $\theta = 60°$ and $\varphi = 60°$. The permittivity and conductivity tensors are

$$\boldsymbol{\varepsilon}' = \varepsilon_0 \begin{pmatrix} 3.250 & 0.217 & 0.375 \\ 0.217 & 2.438 & 0.758 \\ 0.375 & 0.758 & 3.313 \end{pmatrix} \quad \boldsymbol{\sigma}' = \begin{pmatrix} 0.043 & 0.002 & 0.004 \\ 0.002 & 0.034 & 0.008 \\ 0.004 & 0.008 & 0.043 \end{pmatrix} \tag{4}$$

The backscattering RCS of the anisotropic plate are shown in Figure 3(b). The real and broken lines denote that the angle α are 0° and 90°, respectively. The backscattering RCS of the anisotropic plate have obviously resonance characteristic. This characteristic can be used to reconstruct the transverse parameters of the anisotropic plate.

4. RECONSTRUCTION OF TRANSVERSE PERMITTIVITY FOR A LOSSY ANISOTROPIC PLATE

The reflection and transmission of an infinite isotropic slab have resonance characteristic when the thickness of the slab is equal to integral times of a quarter wavelength in medium, namely,

$$d = \lambda m/4 = vm/(4f) = mc_0/(4f\sqrt{\varepsilon_r \mu_r}), \quad m = 1,\, 2,\, 3,\, \ldots \tag{5}$$

in which d, f, v, λ, c_0, ε_r and μ_r are the thickness of the slab, incident wave frequency, wave velocity in medium and wavelength in medium, the EM wave velocity in vacuum, relative permittivity and relative permeability of the medium, respectively. Consider the half-cycle reflection phase shift, the reflectance is local minimum when m are even numbers and the reflectance is local maximum when m are odd numbers. If the medium is no magnetism, namely, $\mu_r = 1.0$,

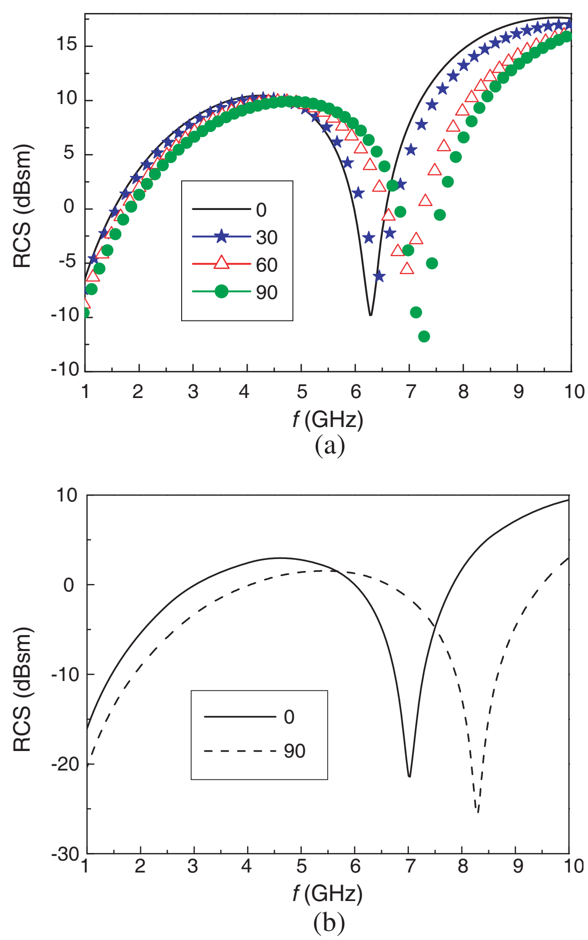

Figure 3. The backscattering RCS of an anisotropic plate. (a) Principal system and laboratory system are superposition, (b) principal system and laboratory system are not superposition.

Equation (5) can be written as

$$\varepsilon_r = \left[(mc_0) / (4fd)\right]^2 \quad m = 1,\, 2,\, 3,\, \ldots \tag{6}$$

Based on the resonance characteristics of the backscattering RCS, the permittivity of an isotropic medium can be reconstructed by using Equation (6). The numerical results show the reconstructed results using the resonance frequency of local minimum is better than using the resonance frequency of local maximum. So the permittivity is reconstructed by using the local minimum resonance frequency in this paper.

Then the Equation (6) is extended to reconstruct the transverse parameters of an anisotropic medium. The reconstructed results of Figure 3(a) are shown in Table 1. In Figure 3(b), the resonance frequency (local minimum) of the real line is $f_1 = 7.032\,\text{GHz}$, and the resonance frequency (local minimum) of the broken line is $f_2 = 8.277\,\text{GHz}$. The relative permittivity of the real and broken lines are $\varepsilon'_{xx} \approx 3.16$ and $\varepsilon'_{yy} \approx 2.28$, respectively. The theory values of the permittivity of the real and broken lines are 3.25 and 2.44, and the relative errors are 2.8% and 6.6%, respectively. It is remarkable that the conductivity can influence the velocity of EM wave in the medium, and also influence the precision of Equation (6). The numerical results show that the transverse parameter of the anisotropic plate can be reconstructed by using Equation (6) when the conductivity is small.

Table 1. Resonance frequency and the reconstructed results.

α	f_r(GHz)	ε_r		Relavively error
		Theory value	Reconstruction results	
0° (real line)	6.27	**4.00**	3.97	0.75%
30° (★)	6.45	**3.77**	3.76	0.27%
60° (Δ)	6.93	**3.28**	3.25	0.91%
90° (•)	7.23	**3.00**	2.99	0.33%

5. BACKSCATTERING CHARACTERISTICS OF THE UNIAXIAL MEDIUM IN LABORATORY SYSTEM

It is worth noting that the backscattering RCS of the uniaxial plate has no cross polarization component in principal system when the EM wave incident along x, y or z axes and the electric field is polarization along one of the two other axes. To find an appropriate way to reconstruct the principal axis for uniaxial material, we take three sample plates of the same size, which are cut perpendicularly to x', y', and z' axes in the laboratory coordinate system. The three sample plates are parallel to $y'o'z'$ plane (Sample plate I), $x'o'z'$ (Sample II) and $x'o'y'$ (Sample III), respectively. Suppose the incident waves along x', y', or z' axis are perpendicular to each of the three sample plates. Considering the permittivity tensor Equation (3) in laboratory coordinate system, the backscattering characteristics of uniaxial plate in laboratory coordinate system are listed in Table 2.

Table 2. Backscattering characteristics of the uniaxial medium in laboratory system.

sample	Incident wave		*D* in the sample	Cross polarization component of back scattering RCS
	Incident direction	*E*-Polarized		
Sample I	x' axis	along y' axis, $E_{y'} \neq 0$	$D_{y'} \neq 0$, $D_{z'} \neq 0$	Yes
		along z' axis, $E_{z'} \neq 0$	$D_{y'} \neq 0$, $D_{z'} \neq 0$	
Sample II	y' axis	along x' axis, $E_{x'} \neq 0$	$D_{x'} \neq 0$, $D_{z'} = 0$	No
		along z' axis, $E_{z'} \neq 0$	$D_{x'} = 0$, $D_{z'} \neq 0$	
Sample III	z' axis	along x' axis, $E_{x'} \neq 0$	$D_{x'} \neq 0$, $D_{y'} = 0$	No
		along y' axis, $E_{y'} \neq 0$	$D_{x'} = 0$, $D_{y'} \neq 0$	

6. RECONSTRUCTING THE PRINCIPAL AXIS FOR UNIAXIAL MEDIUM IN LABORATORY COORDINATE SYSTEM

According to Table 2, x' axis can be determined from backscattering measurement of cross polarization component, which is perpendicular to Sample I. In order to figure out the principal z axis, we denote the direction perpendicular to Sample II and III as u and v directions, respectively, as shown in Figure 4. Then we are going to determine the two angles of principal axes with respect to u and v directions, respectively. With these two angles obtained, the principal z axis can be completely determined. While we choose u direction as positive z' axis, and denote θ as the angle of z' axis with respect to principal axis

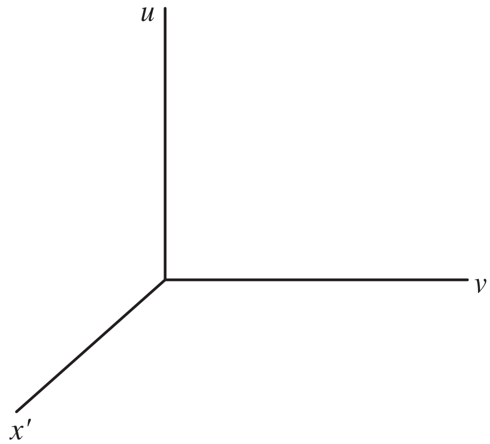

Figure 4. Three orthogonal directions in laboratory coordinate system.

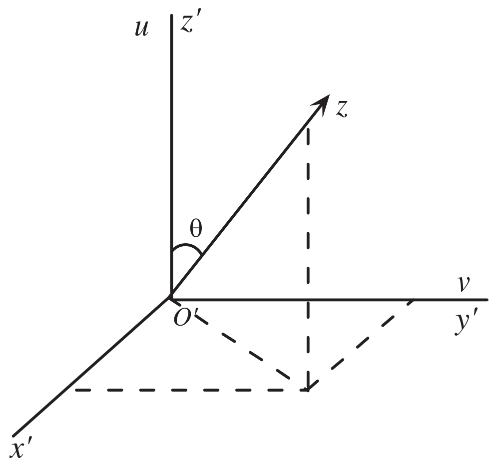

Figure 5. Choose u direction as the positive z' axis.

z, as shown in Figure 5, the relative permittivity tenor is written as

$$\boldsymbol{\varepsilon}' = \begin{bmatrix} \varepsilon & 0 & 0 \\ 0 & \varepsilon_{yy} & \varepsilon_{yz} \\ 0 & \varepsilon_{zy} & \varepsilon_{zz} \end{bmatrix} \tag{7}$$

in which ε_{yy}, ε_{zz} and ε can be reconstructed by the resonance characteristics of the backscattering RCS. The parameters ε_z and θ are still unknown. The relationship between θ and element of the relative permittivity tensor can be obtained from Equations (3) and (7),

$$\varepsilon_z = (\varepsilon_{yy} + \varepsilon_{zz}) - \varepsilon \quad \theta = \arcsin\left(\sqrt{(\varepsilon_{yy} - \varepsilon)\,/\,(\varepsilon_z - \varepsilon)}\right) \tag{8}$$

while we choose v direction as the negative z' axis, the angle of positive z axis with respect to negative z' direction is θ', as shown in Figure 6; the relative permittivity tenor in laboratory system is

$$\boldsymbol{\varepsilon'} = \begin{bmatrix} \varepsilon & 0 & 0 \\ 0 & \varepsilon'_{yy} & \varepsilon'_{yz} \\ 0 & \varepsilon'_{zy} & \varepsilon'_{zz} \end{bmatrix} \tag{9}$$

in which ε'_{yy}, ε'_{zz} and ε can be reconstructed by the same token as above. We have

$$\varepsilon_z = \left(\varepsilon'_{yy} + \varepsilon'_{zz}\right) - \varepsilon \quad \theta' = \arcsin\left(\sqrt{\left(\varepsilon'_{yy} - \varepsilon\right)\,/\,(\varepsilon_z - \varepsilon)}\right) \tag{10}$$

which is similar to Equation (5) except the coordinate system is set as in Figure 6 instead of in Figure 5.

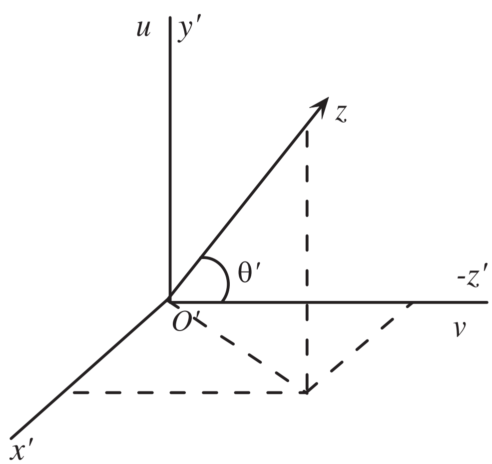

Figure 6. Choose v direction as the negative z' axis.

In a word, in laboratory system, when choose the positive z' axis as u direction, the angle between positive z axis and positive z' axis and the angle between positive z axis and positive y' axis are θ and θ', respectively. Then the principal axis (z axis) of the uniaxial medium is reconstructed in laboratory coordinate system. With these two angles determined, we may obtain the angle φ via the relationship $\sin\theta\cos\varphi = \cos\theta'$.

7. NUMERICAL RESULTS

[**Example 1**] The backscattering of a uniaxial plate when angle θ is changed.

Suppose the relative permittivity tensor of the principal system is $\boldsymbol{\varepsilon}_r = \text{diag}\,(2.0,\, 2.0,\, 4.0)$. The dimension of the sample plate is $0.363\,\text{m} \times 0.363\,\text{m} \times 0.042\,\text{m}$ (Sample I, II and III have the same dimension), and the angle θ is 30°. The backscattering RCS of Sample I plate and Sample III plate when the incident wave are perpendicular to the sample plane are shown in Figure 7 and Figure 8, respectively. In Figure 7 and Figure 8, the real line, circle and broken line denote the electric field polarization along x', y' and z' axes, respectively. The backscattering RCS have not evident cross polarization component as shown in Figure 7 and Figure 8.

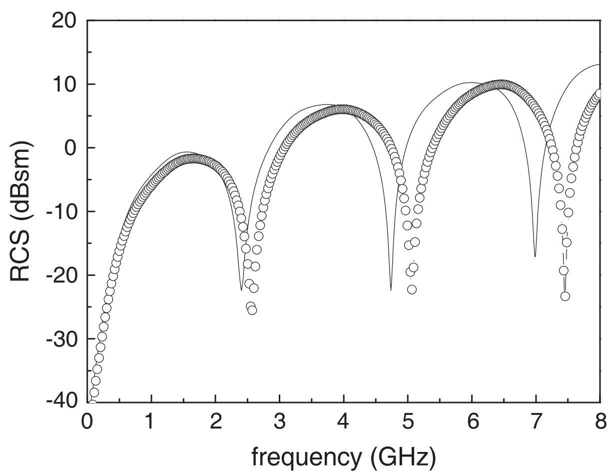

Figure 7. The backscattering RCS of Sample I ($\theta = 30°$).

The backscattering RCS of the Sample II when the wave incident along the x' axis is shown in Figure 9; the broken line and circle have the same meaning as in Figure 8; the triangle and the dot indicate the cross polarization backscattering RCS when the electric field polarization along z' and y' axes.

The cross backscattering RCS of the Sample II when angle θ is changed are shown in Figure 10. The "+", star, triangle, circle and dot denote the case θ are 1°, 2°, 5°, 15° and 30°, respectively. The backscattering RCS when the electric field polarization along y' (real line) and z' (broken line) of Sample II with angle $\theta = 1°$ are shown in Figure 10 for comparison. With the decreasing of the angle θ the cross backscattering RCS of Sample II decrease. There are evident cross backscattering RCS which can be easily detected even if the angle is small as $\theta = 1°$.

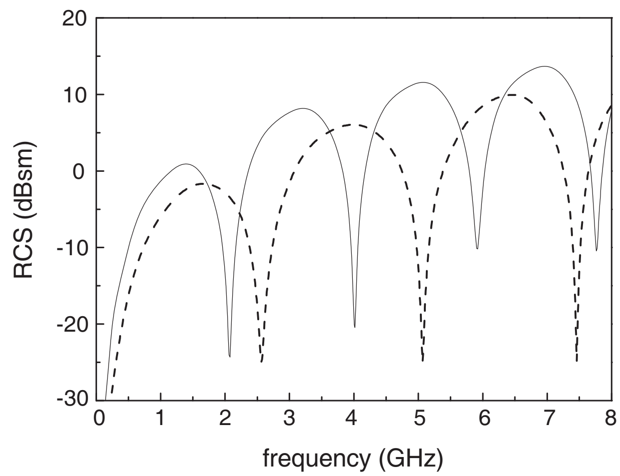

Figure 8. The backscattering RCS of Sample III ($\theta = 30°$).

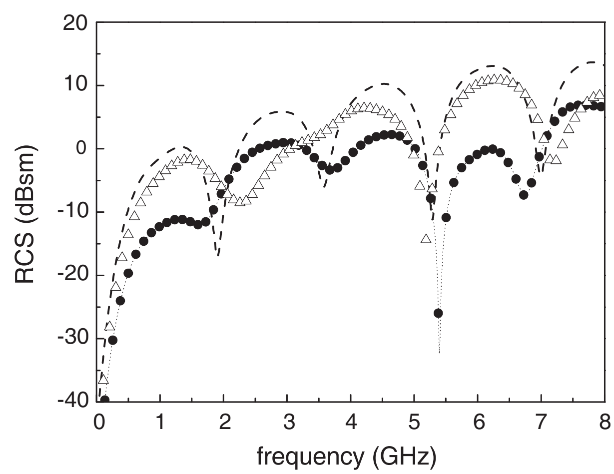

Figure 9. The backscattering RCS of Sample II ($\theta = 30°$).

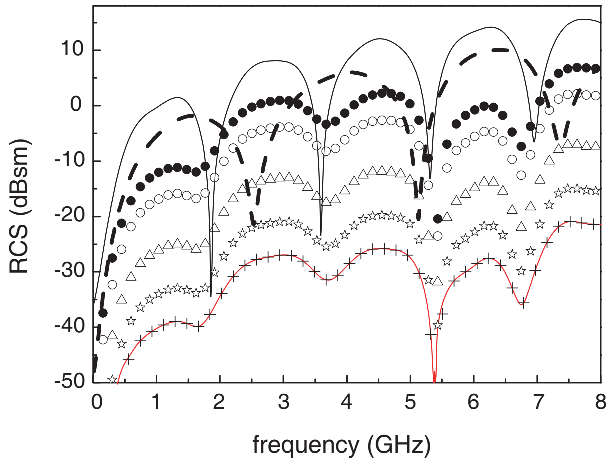

Figure 10. The backscattering RCS of Sample II (θ is different).

[**Example 2**] Reconstructing the principal axis and permittivity tensor for uniaxial medium in laboratory coordinate system.

Suppose the relative permittivity tensor in the principal system is $\boldsymbol{\varepsilon}_r = \text{diag}\,(4.0,\ 4.0,\ 4.3)$. The dimension of sample plate is $0.402\,\text{m} \times 0.402\,\text{m} \times 0.01\,\text{m}$ (Sample I, II and III have the same size). The orientation angles of principal axis (z axis) described in laboratory coordinate system are $\theta = 45°$ and $\varphi = 45°$, i.e., the angle of z axis with respect to z' axis is $45°$, and the angle of z axis with respect to y' axis is $\theta' = 60°$, because of $\sin\theta\cos\varphi = \cos\theta'$. The results computed by FDTD method show that Sample plate I has cross polarization component of backscattering RCS that is independent of the polarization of incident wave. Choose the direction perpendicular to Sample I plane as x' axis, the rest two directions denoted as u and v direction, respectively, as shown in Figure 4.

The backscattering RCS of the sample plate when choose z' axis as u direction are shown in Figure 11; the "star" (resonance frequency is 7.47 GHz), "triangle" (resonance frequencies is 7.33 GHz) and "circle" (resonance frequencies is 7.33 GHz) denote the Case 1: the incident wave is perpendicular to $x'o'y'$ plane with electric field polarized in x' and y' axis, and the Case 2: the incident wave is perpendicular to $x'o'z'$ plane with electric field polarized in z' axis, respectively. By performing the constitutive parameter reconstruction procedure as above, we obtain that $\varepsilon_{xx} = 4.03$, $\varepsilon_{yy} = 4.19$ and $\varepsilon_{zz} = 4.19$. Noting that $\varepsilon = \varepsilon_{xx} = 4.03$ in the principal system, we can obtain from Equation (5) $\varepsilon_z = 4.35$ and $\theta = 45.0°$.

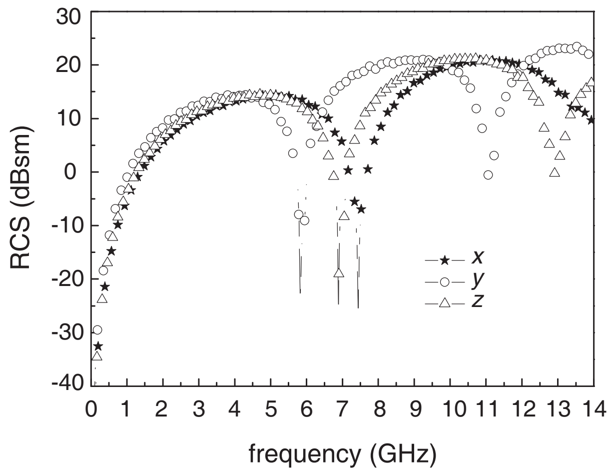

Figure 11. The backscattering RCS when choose the positive z' axis as u direction.

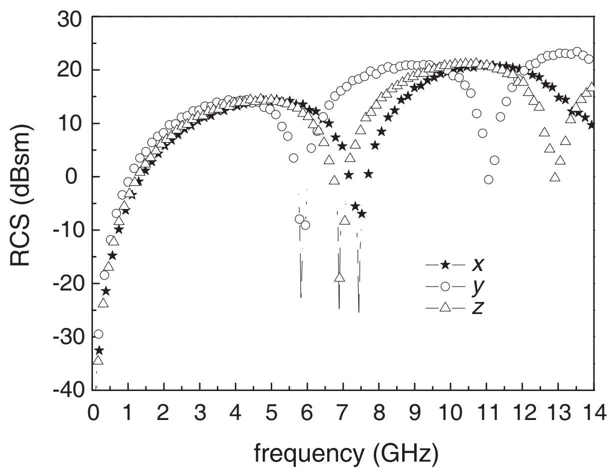

Figure 12. The backscattering RCS when choose the negative z' axis as v direction.

The backscattering RCS of sample plate while we choose v direction as $-z'$ axis as shown in Figure 12, the "star" (resonance frequency is 7.47 GHz), "triangle" (resonance frequencies is 7.26 GHz) and "circle" (resonance frequencies is 7.55 GHz) denote Case 1: the incident wave is perpendicular to $x'o'y'$ plane with electric field polarized in x' and y' axis, and Case 2: the incident wave is perpendicular to $x'o'z'$ plane with electric field polarized in z' axis, respectively. Again, by performing the constitutive parameter reconstruction procedure as above, we obtain $\varepsilon'_{xx} = 4.03$, $\varepsilon'_{yy} = 4.27$ and $\varepsilon'_{zz} = 3.94$. Noting that $\varepsilon = \varepsilon'_{xx} = 4.03$ in the principal system, we can obtain from Equation (7) $\varepsilon_z = 4.17$ and $\theta' = 54.8°$.

Based on the above results, we have $\theta = 50.0°$ and $\theta' = 54.8°$, or $\theta = 45.0°$ and $\varphi = \cos^{-1}(\cos\theta'/\sin\theta) = 54.8°$. The reconstructed result of the element of the relative permittivity ε and ε_z are $\varepsilon = 4.03$ and $\varepsilon_z = 4.20$. The relative reconstruction errors are 0.0% and 8.7%, respectively. The numerical results show the RCS of the anisotropic sample plate can be influenced by the edge effects, but the local minimum of reflectance is basically unchanged when the dimension of the plate is changed (if the thickness of the sample plate is unchanged). So the reconstructed results are basically not influenced by the edge effects.

8. CONCLUSION

In this paper, a new reconstruction scheme of principal axis and permittivity tensor for uniaxial medium via the backscattering measurement in free space is presented when the laboratory coordinate system is adopted. By using three sample plates cut perpendicularly with each other in the laboratory system and measuring the backscattering RCS of the plates in wide band with different polarization status, the principal axis and permittivity tensor can be determined. Numerical simulation demonstrates the availability of presented scheme.

ACKNOWLEDGMENT

This work is supported by the National Natural Science Foundation of China (Grant No. 60871071) and the National Natural Science Foundation for Post-doctoral Scientist of China (Grant No. 20070421109).

REFERENCES

1. Wang, M. Y., J. Xu, J. Wu, B. Wei, H.-L. Li, T. Xu, and D.-B. Ge, "FDTD study on wave propagation in layered structures with biaxial anisotropic metamaterials," *Progress In Electromagnetics Research*, PIER 81, 253–265, 2008.
2. Liu, S.-H., C.-H. Liang, W. Ding, L. Chen, and W.-T. Pan, "Electromagnetic wave propagation through a slab waveguide

of uniaxially anisotropic dispersive metamaterial," *Progress In Electromagnetics Research*, PIER 76, 467–475, 2007.

3. Ding, W., L. Chen, and C.-H. Liang, "Characteristics of electromagnetic wave propagation in biaxial anisotropic left-handed materials," *Progress In Electromagnetics Research*, PIER 70, 37–52, 2007.
4. Gong, Z. and G. Q. Zhu, "FDTD analysis of an anisotropically coated missile," *Progress In Electromagnetics Research*, PIER 64, 69–80, 2006.
5. Kristensson, G., S. Poulsen, and S. Rikte, "Propagators and scattering of electromagnetic waves in planar bianisotropic slabs — An application to frequency selective structures," *Progress In Electromagnetics Research*, PIER 48, 1–25, 2004.
6. Bass, F. and L. Resnick, "The electromagnetic-wave propagation through a stratified inhomogeneous anisotropic medium," *Progress In Electromagnetics Research*, PIER 48, 67–83, 2004.
7. Zheng, L. G. and W. X. Zhang, "Analysis of bi-anisotropic Pbg structure using plane wave expansion method," *Progress In Electromagnetics Research*, PIER 42, 233–246, 2003.
8. Zhang, M., T. S. Yeo, L. W. Li, and M. S. Leong, "Electromagnetic scattering by a multilayer gyrotropic bianisotropic circular cylinder," *Progress In Electromagnetics Research*, PIER 40, 91–111, 2003.
9. Zhang, M., L. W. Li, T. S. Yeo, and M. S. Leong, "Scattering by a gyrotropic bianisotropic cylinder of arbitrary cross section: An analysis using generalized multipole technique," *Progress In Electromagnetics Research*, PIER 40, 315–333, 2003.
10. Wei, B. and D. B. Ge, "Scattering by a two-dimensional cavity filled with anisotropic medium," *Waves in Random Media*, Vol. 13, No. 4, 223–240, 2003.
11. Zheng, H.-X., X.-Q. Sheng, and E. K.-N. Yung, "Computation of scattering from anisotropically coated bodies using conformal FDTD," *Progress In Electromagnetics Research*, PIER 35, 287–297, 2002.
12. Chen, H. T., G. Q. Zhu, and S. Y. He, "Using genetic algorithm to reduce the radar cross section of three-dimensional anisotropic impedance object," *Progress In Electromagnetics Research B*, Vol. 9, 231–248, 2008.
13. Yang, L. L., D. B. Ge, and B. Wei, "An equivalent anisotropic coating technique based on dyadic surface impedance boundary condition," *Chinese Journal of Electronics*, Vol. 14, No. 4, 712–

716, 2005.

14. Huang, P. K. and H. C. Yin, "Equivalent currents on an anisotropic material backed by a metal surface and their relation," *Journal of Systems Engineering and Electronics*, Vol. 11, No. 4, 1–10, 2000.
15. Yin, H. C., Z. M. Chao, and Y. P. Xu, "A new free-space method for measurement of electromagnetic parameters of biaxial materials at microwave frequencies," *Microwave and Optical Technology Letters*, Vol. 46, No. 1, 72–78, Jul. 5, 2005.
16. Valagiannopoulos, C. A., "On measuring the permittivity tensor of an anisotropic material from the transmission coefficients," *Progress In Electromagnetics Research B*, Vol. 9, 105–116, 2008.
17. Chen, X., T. M. Grzegorczyk, and J. A. Kong, "Optimization approach to the retrieval of the constitutive parameters of slab of general bianisotropic medium," *Progress In Electromagnetics Research*, PIER 60, 1–18, 2006.
18. Fedorov, F. I., G. N. Borzdov, and L. M. Barkovskii, "Operator for the indices of refraction of plane waves in dispersive anisotropic media," *Journal of Applied Spectroscopy*, Vol. 43, No. 4, 1176–1182, 1985.
19. Borzdov, G. N., "An intrinsic tensor technique in Minkowski space with applications to boundary value problems," *J. Math. Phys.*, Vol. 34, No. 7, 3162–3196, 1993.
20. Kong, J. A., *Electromagnetic Wave Theory*, High Education Press, 2002.
21. Taflove, A. and S. C. Hagness, *Computational Electrodynamics — The Finite Difference Time Domain Method*, 3rd edition, Artech House, 2005.
22. John, S. and H. Scott, "The finite-difference time-domain method applied to anisotropic material," *IEEE Trans. Antenna Propag.*, Vol. 41, No. 7, 994–999, 1993.